AN ANALYTICAL MODEL FOR PREDICTING CRACK PROPAGATION IN FRACTURE OPENING MODE (MODE-I)

A. K. El-Senussi
Aeronautical Engineering Department
Al-Fateh University, Tripoli- Libya
E-mail: elsen2005@yahoo.com

الملخص

معظم حالات الانهيار الناجم عن التصدع تعزى إلى الحالة–1. هذا السلوك تحتمه عادة طريقة استعمال الإنشاءات لكي تؤدي غرض محدد. تحتوي هذه الورقة على نموذج تحليلي جدير بالثقة يمثل عينة مدببة عرضياً ذات ذراعين متماثلين حول خط التصدع لغرض دراسة التصدعات المستقرة في حالة الانفتاح (حالة–1). النموذج يأخذ في الاعتبار الإزاحة الرأسية على طول خط التحميل الناتجة من التشوهات في ما بعد رأس التصدع. هذه التشوهات الواقعة في المنطقة غير متصدعة تمكن كل ذراع من ذراعي العينة من الدوران حول قاعدته الطرفية الثابتة مسببة إزاحة رأسية بالإضافة إلى تلك المقدمة من عمليات الثني أو القص.

النموذج يتفق بصورة ممتازة مع النتائج المعملية المنشورة في نطاق تصدع طوله 70% من طول العينة. هذا التطابق المعملي مع التوقعات النظرية المعروفة في هذه الورقة يجعل من هذا النموذج أداة فعَالة في دراسة سريان التصدعات في مسائل الكلال ذات العلاقة بالتكامل.

ABSTRACT

The majority of fracture failure problems are attributed to the opening mode (Mode-I). This feature is mainly imposed by the way constructions are employed to fulfill a particular job.

A simple and reliable analytical model representing a tapered double cantilever beam (TDCB) is presented for studying stable crack propagation in the opening mode (Mode-I). The model accounts for the end deflection associated with deformations beyond the crack tip. Deformation of the uncracked portion allows each arm of the TDCB to rotate about the built-in end, producing an end deflection in addition to those caused by bending and shear. The model agrees very well with published experimental results for a crack to specimen lengths up to 70%. The good agreement of the measured values with the theoretical predictions makes this model a potential tool for studying crack propagation in corrosion fatigue problems.

KEYWORDS: Analytical model, Crack propagation, Opening mode (Mode-1), Double cantilever Beam test specimen.

MATHEMATICAL MODEL

A mathematical model for studying crack propagation was developed in [1]. It consisted of a double cantilever beam (DCB) with straight arms as shown in Figure 1. The elastic strain at the root of the cantilever are taken into account in calculating the

end deflection along the load line. The total vertical displacement for one arm of the DCB is [1].

$$\delta = \frac{4Pa^3}{Ebh^3} + \frac{8.212Pa^2}{Ebh^2} + \frac{1.5Pa}{bhG} \tag{1}$$

where the first and the third terms represent ordinary bending and shear deflections respectively, while the second term is associated with deformations beyond the crack tip as explained in [1].

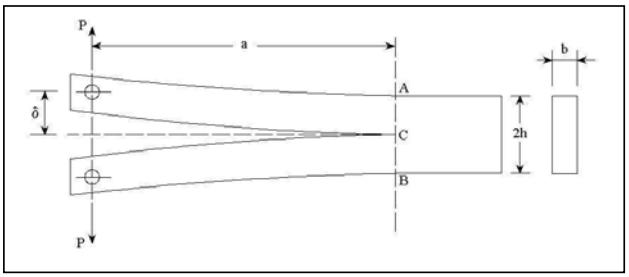

Figure 1: Double Cantilever Beam (DCB); geometry and loading.

In this paper the model is extended to other double cantilever beam configurations. One of these; namely the tapered double cantilever beam specimen (TDCB) (Figure 2), is of particular interest because it can offer a linearly varying compliance C with the crack length a. This can be very useful, because testing may be simplified considerably, while the critical energy release rate g_c is being measured for a certain material. In fact a constant dC/da allows the operator to monitor only the critical load P_c at the onset of crack propagation without being concerned with the crack length unlike the parallel-arm DCB specimen where P_c and a, must be monitored simultaneously. The TDCB specimen can also give slow and stable crack propagation; a feature desired in many test situations. Previously, the TDCB specimen was used, as pointed out in [2], in fatigue studies and environmental cracking investigations. Convenient use of the specimen has also been found in the study of crack propagation characteristics in adhesive joints, and delamination behavior in laminated composites [3].

In Figure 2, there are shown two TDCB versions. The first (Figure 2a) has been widely employed unlike the second where only very limited use is reported in the literature. In fact the author is only aware of the work of Mai et al. [2] where a specimen of the latter type was used. The authors [2] employed a PMMA TDCB specimen as shown in Figure 2b, found that it gave better control of crack path and stability of crack over the TDCB configuration shown in Figure 2a. In this paper the analysis will be limited to the *TDCB* specimen represented in Figure 2a.

With reference to Figure 2a, the total deflection δ given by Eqn. (1) can be easily modified to accommodate the effect of the taper angle θ. The second and third terms in the right hand side of Eqn. (1) are changed through the replacement of the *DCB* arm depth h by the variable arm depth of the TDCB, $h_a=(a+e)\lambda$; where λ is the slope of the

taper and, e, is the distance between the load line and the apex of the specimen as given in Figure 2a.

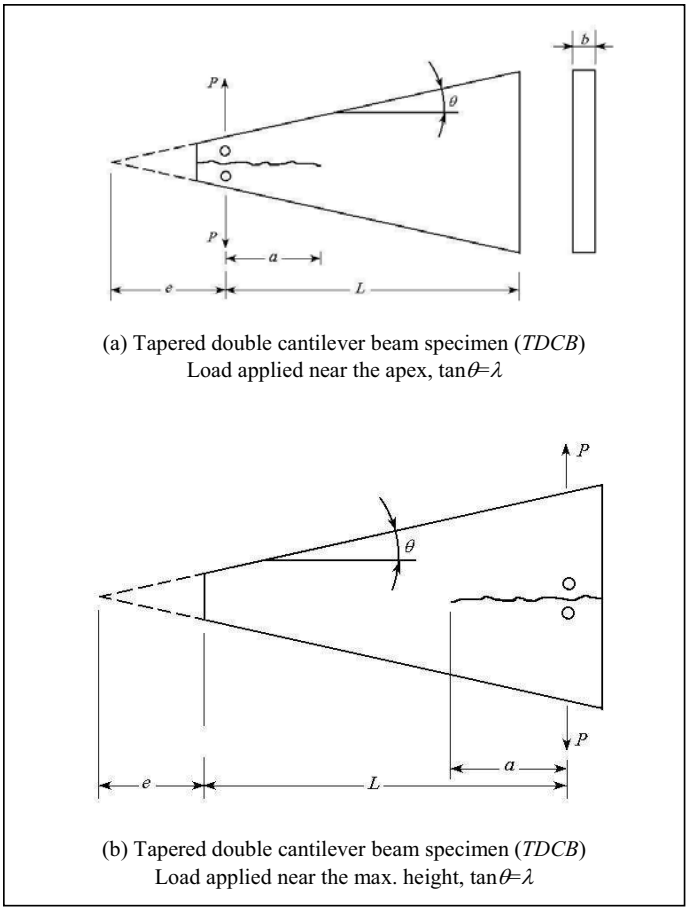

Figure 2: Tapered double cantilever beam specimen (*TDCB*); configuration and loading.

Assuming a small taper angle θ, the simple bending deflection represented by the first term in the right hand side of Eqn. 1 can be replaced by the corresponding expression for the taper shape [2], i.e.,

$$\delta_b = \frac{12P}{Eb\lambda^3}\left[\ln\left(\frac{a+e}{e}\right) + \frac{e(4a+3e)}{2(a+e)^2} - \frac{3}{2}\right] \tag{2}$$

thus, the total arm deflection δ for the *TDCB* is

$$\delta = \frac{12P}{Eb\lambda^3}\left[\ln\left(\frac{a+e}{e}\right) + \frac{e(4a+3e)}{2(a+e)^2} - \frac{3}{2}\right] + \frac{8.212Pa^2}{Ebh_a^2} + \frac{3.75Pa}{Ebh_a} \quad (3)$$

where, E=2.5G, ν=0.25;
therefore, the specimen compliance is given by

$$C = \frac{2\delta}{P} = \frac{24}{Eb\lambda^3}\left[\ln\left(\frac{a+e}{e}\right) + \frac{e(4a+3e)}{2(a+e)^2} - \frac{3}{2}\right] + \frac{16.424}{Eb}\left(\frac{a}{h_a}\right)^2 + \frac{7.5}{Eb}\left(\frac{a}{h_a}\right) \quad (4)$$

In Figure 3 the compliance, C, is plotted versus the crack length, a, for various taper slopes. These graphs show that beyond a crack length of 20mm the behavior of, C, is approximately linear. As already stated earlier, a linear varying compliance is beneficial, in that it gives a constant dC/da. On the other hand, the value of, λ, should not go beyond the validity of the simple theory of flexure.

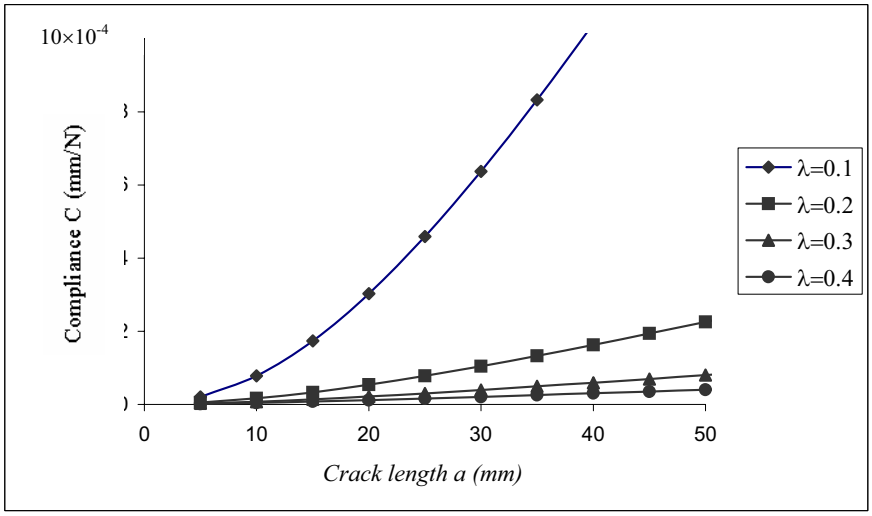

Figure 3: TDCB Compliance versus crack length

The strain energy release rate for the *TDCB* specimen can be obtained from the following equation [4].

$$g = \frac{dU}{d(ab)} = \frac{p^2}{2b}\left(\frac{dc}{da}\right) \quad (5)$$

Substitution from Eqn. (4) into Eqn. (5) yields

$$g = \frac{p^2}{Eb^2h_a^2}\left[\frac{12a^2}{h_a} + 16.424e\lambda\left(\frac{a}{h_a}\right) + 3.75e\lambda\right] \quad (6)$$

In terms of the stress intensity factor K_I this equation becomes ($K_I^2 = Eg$);

$$\frac{K_I b h_a^{\frac{1}{2}}}{P} = 2\sqrt{3}\left[(1-1.37\lambda)\left(\frac{a}{h_a}\right)^2 + (1.37-0.313\lambda)\left(\frac{a}{h_a}\right) + 0.313\right]^{\frac{1}{2}} \quad (8)$$

The stress intensity factor coefficient $K_I b h_a^{\frac{1}{2}} \Big/ P$ is plotted in Figure (4) for various values of λ. It is seen that the lines form a bunch like shape. These are entirely linear for relatively small tapers, and they depart gradually from linearity near $a/h_a = 0$ as the taper is increased. For the range of taper considered the lines meet the (a/h_a)-axis at $(a/h_a) \cong -0.685$. Therefore, for small tapers we may write;

$$\frac{K_I b h_a^{\frac{1}{2}}}{P} = \psi\left(\frac{a}{h_a} + 0.685\right) \quad (9)$$

where ψ is a λ-dependent function representing the slopes of the lines shown in Figure (4). Srawley and Gross [5] found, from their boundary collocation analysis, that the intercept $a/h_a = 0.7$. Srawley and Gross [5] derived the following formula from fitting their elasticity results to a set of straight lines such as those shown in Figure (4)

$$\frac{K_I b h_a^{\frac{1}{2}}}{P} = \Lambda\left(\frac{a}{h_a} + 0.7\right) \quad (10)$$

where Λ is a taper dependent implicit function which represents the slopes of the lines in the $K_I b h_a^{\frac{1}{2}} \Big/ P$ versus a/h_a graphs of [5]. The suspicion of Srawley and Gross that the linear relation Eqn. (10) would not apply to actual specimens with small a/h_a (i.e., higher taper angle), is confirmed by the results shown in Figure (4) wherein a departure from linearity can be detected as λ grows bigger. An attempt to estimate the factor ψ in Eqn. (9), by comparing the compliance C given by Eqn. (4), and another corresponding expression obtained through integration from combining Eqns. (5) and (9) with the relation $K_I^2 = Eg$ gives

$$\psi = 2\sqrt{3}(1 + 1.37\lambda + 0.47\lambda)^{-\frac{1}{2}} \quad (11)$$

Besides its simplicity, Eqn. (9) follows quite well the graphs shown in Figure (4) for $\lambda \le 0.4$.

Let us recall one particular assumption which remains at the origin of the present analysis; the specimen containing the crack has a semi-infinite uncracked portion beyond the crack tip. In practice, the double cantilever beam specimen has finite dimensions and, therefore, we are bound to explain how much length the uncracked portion would have before the end hinge effects are felt. Srawley and Gross [5] approached the problem and identified two hinge-affected and non affected regions within the specimen, depending on the range of *a/L*; where *a/L* is the ratio of the crack length to the distance between the load line and the specimen base ahead of the crack tip [see Figure 2a]. Their conclusions are:

1. for a/L < 0.7 ; the dimensionless stress intensity factor, $K_I b h_a^{\frac{1}{2}} / P$, follows Eqn. (10), and
2. for a/L ≥ 0.7, the behavior is governed by the following equation, which the authors [5] obtained by reformulating and adopting Eqn. (181) of [6] so that

$$\frac{P_C}{K_I b L^{1/2}} = \frac{(1-a/L)^{\frac{1}{2}}}{0.537 + 2.17(1+a/L)/(1-a/L)} \tag{12}$$

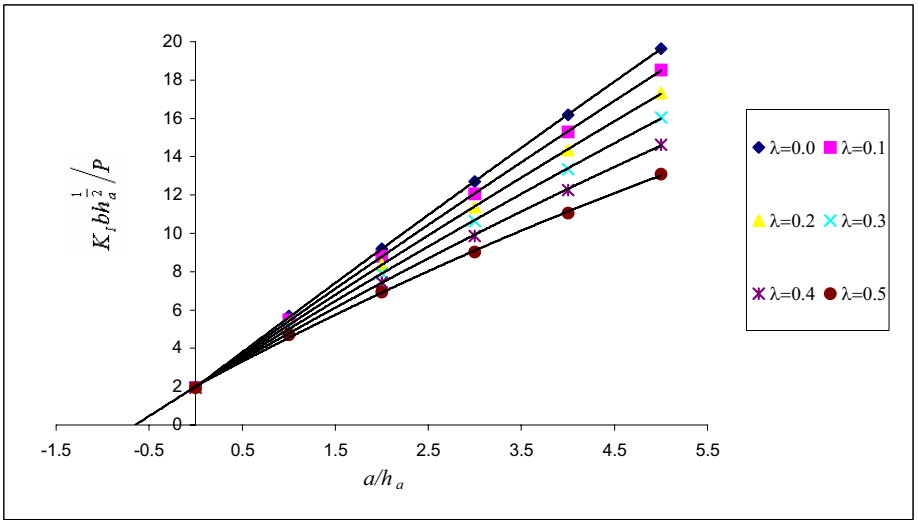

Figure 4: Stress intensity coefficient versus ratio of crack length to TDCB arm height

Let us now examine our theory in the light of above conclusions and the experimental results of Mai, Atkins and Caddell [2] by reformulating Eqn. (6) as follows:

$$\frac{P_C^*}{(ELg_C)^{\frac{1}{2}}} = \frac{\lambda^{3/2}(z+s)^{3/2}}{\left[12z^2 + 16.424sz\lambda + 3.75(z+s)s\lambda^2\right]} \tag{13}$$

where [see Figure 1(a)], $P_C^* = P_C / b$ is the critical applied load per unit width, $s=e/L$ and $z=a/L$.

the dimensionless load coefficient $P_C^* / (ELg_C)^{\frac{1}{2}}$ is plotted versus z in Figure 5 along with the experimental results, for the *PMMA* tapered double cantilever beam test specimens, taken from [2]. The continuous curves in Figure 5. represents Eqn. (13). It is seen from the graphs that the agreement of the present analysis with the experimental data is very good up to a value of *a/L* around 0.7 and, that for higher values of this ratio the experimental data tend to follow Eqn. (12) as concluded by Srawley and Gross [5]. The simplicity and the remarkable agreement with experiments of Eqn. (7) [or

equivalently Eqn. (13)] make this a reliable candidate in future fracture toughness measurement for a certain material.

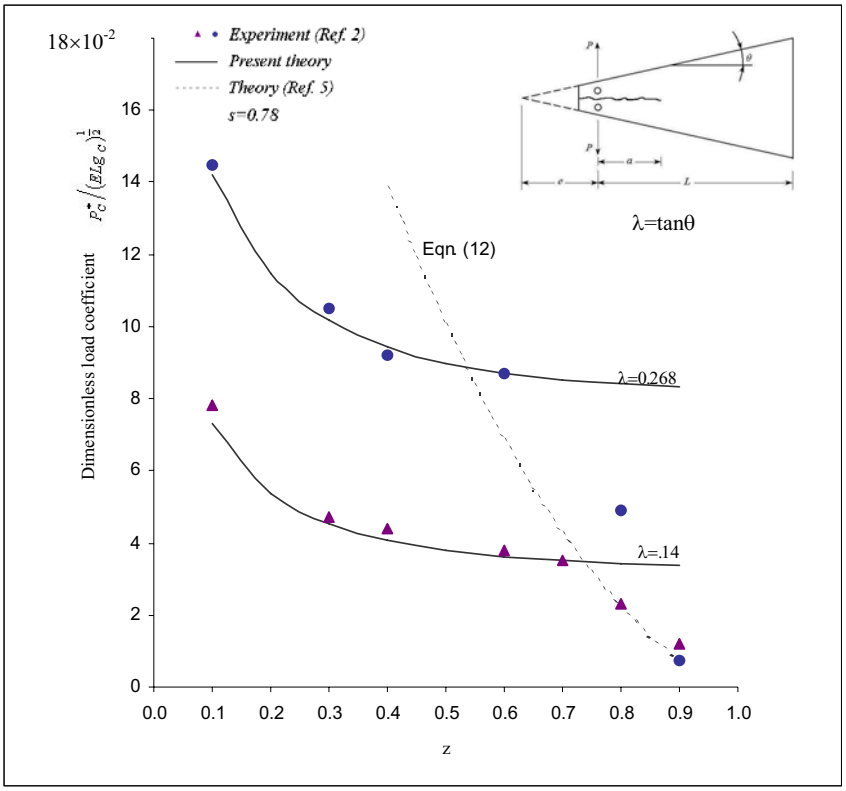

Figure 5: Dimensionless load factor versus the ratio of the crack length to the distance between the load line and the specimen base

CONCLUSION

A simple theoretical analysis based on a realistic model has been established of the load-deflection relationship for the DCB specimen. The strain energy of bending stored in the DCB arms was evaluated and used in formulating expression for the strain energy release rate which can be employed reliably to predict the fracture toughness of a certain material. TDCB dimensionless fracture strength was compared with established experimental data and found to be in very good agreement for values of ratio between crack length and effective specimen length (distance between load line and specimen base) ranging up to 0.7.

REFERENCES

1. El-Senussi, A. K, Webber, J. P., On Double Cantilever Beam Technique for Studying Crack Propagation. J. Appl. Physics, Vol. 56, No. 4, 15 Aug. 1984, pp. 885-889.

2. Mai, Y. W., Atkins, A. G., Caddell, R. M., On the Stability of Cracking in Tapered DCB Test-pieces. Int. J. Fracture, Vol. II, No. 6, Dec. 1975, pp. 969-953.
3. Hopkins, R. B., Design Analysis of Shafts and Beams, McGraw-Hill, Inc, New York, 1970.
4. El-Senussi, A. K, Webber, J. P., Critical Energy Release Rate Delamitation of Carbon Fiber Reinforced Plastic (CFRP) Laminates. COMPOSITES, Vol. 20.N°3. May 1989, pp. 249-256.
5. Strawley, J. E., Gross, B., Stress Intensity Factor for Crack line-load edge-crack Specimens. Materials & Standards, Vol. 7, April 1967, pp. 155-162.
6. Paris, P. C., Sih, G. C., Stress Analysis of Cracks, ASTM STP 381, 1965, pp. 30-83.

NOTATION

a	Crack length
A	Crack surface
B	*DCB* specimen width
C	Compliance
E	Young modulus
e	Distance between load line and *TDCB* apex
g	Energy release rate
g_c	Critical energy release rate
G	Shear modulus
H	*DCB* arm depth
h_a	*TDCB* arm height at crack tip
K_I	Stress intensity factor
L	Distance between load line and *DCB* base
P_C	Critical applied load
P_C^*	Critical applied load /unit width
s	Ratio of apex and base distances from load line
U	Strain energy /unit width
z	Ratio of crack length and base distances from load line
δ	*DCB* arm deflection
δ_b	Bending deflection
δ_s	Shear deflection
$\Delta=2\delta$	Crack mouth spacing displacement
θ	Angle of *TDCB* taper
λ	Slope of taper for *TDCB* specimen
Λ	Taper dependent implicit function
ν	Poisson's ratio
π	Common's constant (=3.141593)

ABBREVIATIONS

DCB	double cantilever beam
PMMA	Polymethylmethacrylate
TDCB	Tapered double cantilever beam